Transmission in one-dimensional channels in the heated electron regime

1989 J. Phys.: Condens. Matter 1 7643

(http://iopscience.iop.org/0953-8984/1/41/016)

J. Phys.: Condens. Matter 1 (1989) 7643–7649. Printed in the UK

Transmission in one-dimensional channels in the heated electron regime

M J Kelly†
Cavendish Laboratory, Madingley Road, Cambridge CB3 0HE, UK

Received 8 June 1989

Abstract. The transmission coefficient is calculated for electrons in a one-dimensional channel when a source–drain potential bias is applied. For large biases (typically greater than the Fermi energy of the electron gas) the transmission drops significantly from unity, which would be manifest in a reduced conductance, or increased resistance, as a source–drain field is applied. A novel form of negative differential resistance is predicted.

1. Introduction

The simple arguments leading to the quantisation of the one-dimensional ballistic resistance (Wharam *et al* 1988, van Wees *et al* 1988) are based on the Landauer (1981, 1985) formula and rely on assuming $tt^* = 1$, where t is the transmission amplitude for an electron wavefunction within the channel: this is typically an electrostatically defined constriction within an otherwise two-dimensional electron gas (see Wharam *et al* (1988) for the experimental device structure). Under weak biases and with degenerate carriers, the current is dominated by electrons near the Fermi energy, and the assumption that $tt^* = 1$ is reasonable. The simple one-dimensional model that gives the quantised resistance has been generalised to consider the fuller two-dimensional aspects of the contacts on either side of the channel, and the coupling of states with different momenta in a direction at right angles to the constriction axis (Szafer and Stone 1988, Kirczenow 1988). The results are qualitatively the same, except for in narrow regions over which the coupling is weak and the net conductance is reduced from the quantised value. The less-than-unity transmission is related to a mismatch of the types of wavefunction in the wide contact regions and the narrow constriction. In this work we describe one-dimensional calculations of another situation where mismatch can occur, i.e. where a source–drain bias results in a significant difference between the bottom of the bands on either side of the constriction, or equivalently the $\boldsymbol{k}$-vectors of the electron states at the same energy on either side differ.

In the first part of the calculation, the problem is set up and one obtains the contribution to the transmission current from electrons incident with different energies at constrictions with different lengths and source–drain biases applied. Two different models are considered for the potential profile within the constriction: one is based on a linear voltage drop, and the other uses a more complicated potential profile that has a

† Also at GEC Hirst Research Centre, East Lane, Wembley, UK.

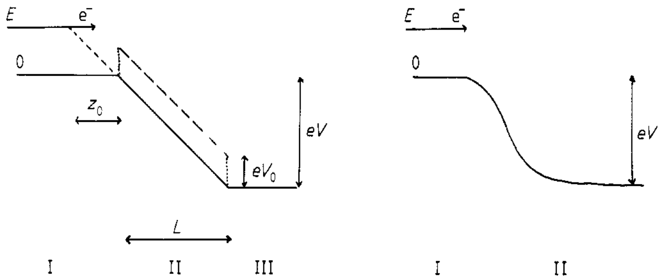

Figure 1. The potential profiles considered here, and the structure for calculating the *J–V* characteristics.

continuous first derivative at the matching point (figure 1). This latter is important as it is likely to be the more applicable to real devices. The results from the former show some length resonance effects that are related to $\int k(z)\,\mathrm{d}z = n\pi$ within the channel, but these are absent in the latter model. In some actual experiments (Brown *et al* 1989), the split gate (see Thornton *et al* (1986) for details) is used to define and ultimately pinch off the channel, with a source–drain bias then being used to force electrons through the constriction. This situation can be modelled relatively easily in the case where the linear-potential drop is assumed (again see figure 1) by raising the potential energy floor in the constriction. The results demonstrate the role of quantum reflection as the source–drain bias increases.

In the second part of the calculation, a sum is performed of the transmission currents appropriate to all electron states incident on the channel to obtain the current–voltage characteristics, and so extract the conductance. This shows an averaging out of the length resonance effects with the linear potential drop in the absence of any pinching off. The reduced transmission as the bias increases leads eventually to a negative differential resistance, some preliminary evidence of which has recently been demonstrated (Kelly *et al* 1989, Brown *et al* 1989).

2. Linear potential drop

Consider a one-dimensional problem in which the bottom of the conduction band is at zero potential for $z < 0$ (region I), and drops linearly (in region II) to a value $-V$ ($V > 0$ in our notation) at a position $z = L$, and remains at this value for $z > L$ (region III). The wavefunctions for an electron of energy E incident from the left can be written as

$$\begin{array}{ll} \text{in region I} & \psi = \exp(\mathrm{i}kz) + r\exp(-\mathrm{i}kz) \\ \text{in region II} & \psi = \alpha\mathrm{Ai}(\xi(z-z_0)) + \beta\mathrm{Bi}(\xi(z-z_0)) \\ \text{in region III} & \psi = t\exp(\mathrm{i}k'z) \end{array}$$

where Ai and Bi are Airy functions, $k = \surd(2m^*E/h^2)$, $k' = \surd[2m^*(E+V)]$, $z_0 = -E/(V/L)$, i.e. the position where the linear potential in the constriction would extrapolate to the energy E, $\xi^3 = -[2m^*e(V/L)/h^2]$ (so ξ has the dimensions of an inverse length), and m^* is the electron effective mass. It is a straightforward matter to equate both ψ and $\delta\psi/\delta z$ and both $z = 0$ and L, and eliminate α, β and r from the above equations. The

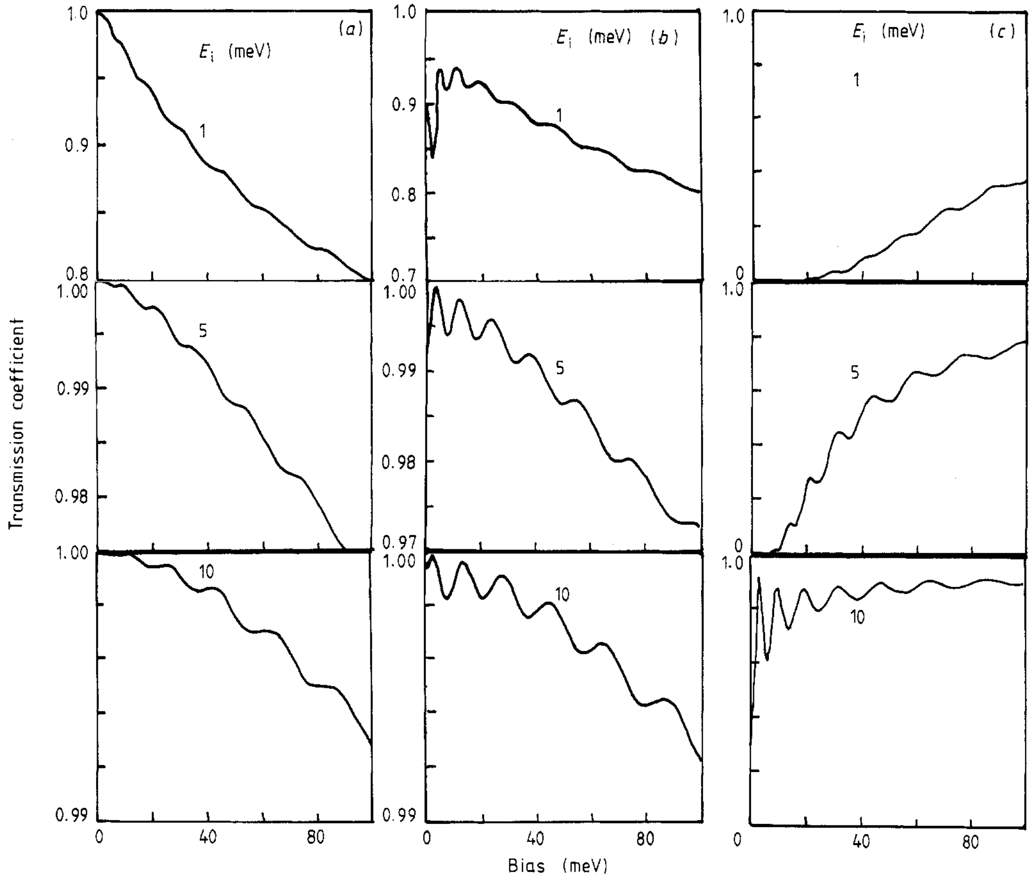

Figure 2. (*a*) The transmission coefficient for electrons of different energy incident on a linear potential drop over a constriction length of 0.1 μm as a function of bias. (*b*) The same as in (*a*), but with the potential floor in the channel raised by 10% of the Fermi energy. (*c*) The same as in (*b*), but with the potential floor raised by 90% of the Fermi energy.

actual formulae derived and used in the calculations are included in the Appendix. The relative current associated with the exiting electron is given by $k'tt^*/k$. We show the results of calculations in figure 2(*a*) for electrons incident with energies of 1, 5 and 10 meV for channels of length 0.1 μm as the bias is increased from 0 to 100 mV, this last being a very large bias in experimental terms: results have been achieved for biases up to these values in samples where the Fermi energy is of order 10 meV.

The notable features in the results are as follows.

(i) A significant drop from unity transmission, especially for lower-energy electrons (i.e. those for which the ratio k'/k is the largest), even to as low as 80%.

(ii) A set of oscillations in the transmission superimposed on the drop just described that are in slightly different positions for different incident energies, but that correspond to extra half-wavelengths of the wavefunction being fitted in along the length of the constriction as the bias increases: since the bias energies are rather larger than the scale of the incident energies, the positions of the maxima depend only weakly on the incident conditions.

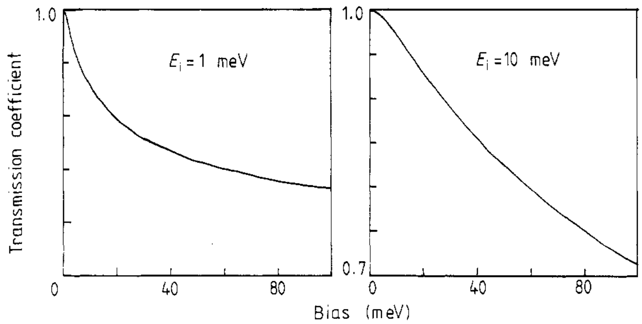

Figure 3. The transmission coefficient for electrons of different energy incident on a smoothly falling potential profile.

(iii) At very low biases, then $tt^* = 1$, and the quantisation is accurate.

(iv) When the constriction is increased to 1 μm in length, the expected differences emerge in the absence of scattering that we assume throughout: first for the same fields the transmission reduction is independent of the length of the constriction, and there are correspondingly more oscillations superimposed on the reduction as more extra half-wavelengths can be fitted in along the contriction.

It is straightforward in this model to add a constant potential $+V_0$ to the potential profile within the length of the contriction, implying a set up in the potential at $z = 0$, and a corresponding step down at $z = L$. The only modification to the above equations is a shift in z_0, and all the remaining methods of solution stay the same. In figures 2(b) and 2(c) the results of figure 2(a) are repeated for values $V_0 = 1$ meV and 9 meV respectively. In the former case, we see a modestly increased deviation from $k'tt^*/k = 1$ for energies well above the barrier, but by the time $V_0 = 9$ meV, i.e. almost equal to the Fermi energy, the reduction is almost total for small biases. In this model we would expect strong reductions in the transmission per channel. This is a crude model for the regime where the electrostatically defined channel is pinched off by a strong negative bias.

3. Smooth potential drop

Consider now an alternative potential profile, namely that $V = 0$ for $z < 0$ (in region I) as before, but now (in region II) for $z > 0$ we have $V(z) = U_0(1/\cosh^2(\alpha z) - 1)$. There is no region III. This potential profile permits 99% of the potential drop over a distance z_0 such that $\alpha z_0 = 2.99$, and we use this length to define the constriction length. The wavefunctions for this potential, which are represented by hypergeometric functions of complicated arguments, are readily available (Landau and Lifshitz 1977), and again the relevant equations are included in the Appendix.

We begin by repeating calculations for the case equivalent to figure 2, and the results are shown in figure 3. Here we obtain an even bigger reduction of the transmission coefficient than that encountered in figure 2(a), but now there are no resonance effects associated with extra half-wavelengths. Both these results are simple to explain: the former related to the fact that the smooth potential allows the differences at $z = 0$ and $z \rightarrow \infty$ to be coupled more strongly, while the latter results from the absence of any

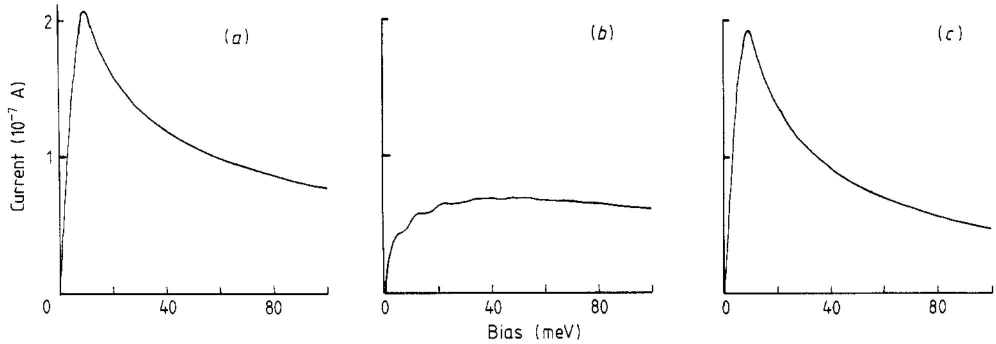

Figure 4. The J–V characteristics for the case of (a), figure 2(a), (b) figure 2(c) and (c) figure 3.

discontinuities in the potential profile or its first derivative. Further calculations show that these differences are independent of the 'length' of the constriction (as defined by α^{-1}). Again these results vindicate the quantisation at small biases, but show that deviations that lead to increased resistances are expected at larger biases.

4. The current–voltage characteristics

Having calculated $t(E_{\text{incident}})$, for different biases, it is a straightforward matter to calculate the current–voltage characteristics in the zero-temperature limit. The current flowing from left to right in figure 1 is calculated as

$$J_{\rightarrow} = e \int \mathrm{d}E\, n(E)v(E)|t(E)|^2$$

where integration is from $E_F - eV$ to E_F if the bias is such that $eV < E_F$, or from 0 to E_F otherwise. In a 1D system, and for each electron spin value, the following relations hold:

$$n(E) = 2\pi\, \mathrm{d}k/\mathrm{d}E \qquad \mathrm{d}E/\mathrm{d}k = hv(E) \qquad n(E) = 1/hv(E)$$

so

$$J_{\rightarrow} = (e/h) \int \mathrm{d}E\, |t(E)|^2.$$

For the sign of bias shown in figure 1, and for low temperatures $J_{\leftarrow} = 0$ for the lack of available final states. (Note that if $t \equiv 1$ then $J = e^2/hV$ and the resistance is quantised: observed deviations from quantised values, in this formalism, are due to deviations from $t \equiv 1$.)

In figures 4(a), 4(b) and 4(c) we have plotted the J–V characteristics for single channels corresponding to the situation in figures 2(a), 2(b) and 3 rspectively. Several points are to be noted. (i) In the absence of any pinching off–i.e. raising the potential floor in the channel—the channel resistance is at its quantised value for $eV \ll E_F$, but already by the time eV is of order 20% of E_F the resistance is beginning to rise from this value. (ii) The oscillating structure in $t(k)$ or $t(E)$ as a function of bias is washed out in the integration for the linear potential drop: only with the introduction of a potential discontinuity in the model for pinching off do these length resonance effects survive, and then only weakly. (iii) As the pinching off occurs, the resistance rises from its quantised value, very slowly at first (we do not reproduce the J–V curve for a 10% pinching off effect, as it is indistinguishable from that with no pinching off), but becoming appreciable once the rise in the potential floor is $\simeq$50% of E_F. (iv) Most notable of all is the fact that once eV exceeds E_F, the differential resistance goes negative: this should lead to current and voltage oscillations within the device. Since we are dealing with resistances of order $10^4\Omega$ and capacitances of order 10^{-18}F, the possible frequencies of such oscillations are extremely high. (The increase in differential resistance, and instabilities in the J–V characteristics have been detected as the bias increases (Brown *et al* 1989).)

5. Discussion

This calculation was initially set up to test the extent to which length resonance features in calculations of conductance were an artefact of discontinuities in the potential profile, or its first derivative (which they are totally). However, the results show a more interesting feature, namely negative differential resistance in the high-source–drain-bias regime.

Provided that the constriction resistance is dominant in the measurement, as is the case in most studies, the effects described above should be clearly observable, although other effects of hot-carrier relaxation such as phonon emission and electron–electron interactions may produce further contributions to the resistance, reducing the magnitude of the effect predicted above. Strictly the equation for the current is § 4 above should contain the Fermi occupation factor $f(E, T)$, and the integral be taken to large positive energy. At finite temperatures there will be a reverse current from partially occupied states on the low-energy side: such a current will be small by a factor of at least $\exp(-eV/kT)$ reflecting the relative occupation of those initial states, and this will result in a small reduction of the magnitude of the negative differential resistance with temperature.

Two theoretical points remain. The first is that our analysis assumes the potential varies strongly on the scale of an electron wavelength: otherwise a WKB-type analysis would result in exponentially small reflections. We note that the Fermi wavelength in the two-dimensional electron gas contact layers is $\simeq 0.05\ \mu$m. In a split-gate structure with multiple sub-band occupation, and part of the kinetic energy taken up as lateral quantum confinement energy, most electrons have wavelengths considerably in excess of this value. For split gates of length $\simeq$0.1–0.3 μm, supporting a potential drop of 20–100 mV, the analysis presented in this paper applies. The second concerns space-charge and screening effects within and near the constriction, and the influence they have on the potential profile seen by the electron. Since the electron density within the constriction is quite low, the simple model in figure 1 is quite appropriate.

Acknowledgments

The work at Cambridge was supported in part by a Royal Society/SERC Industrial fellowship. I have benefited greatly from discussion with R J Brown, M Pepper, D A Wharam, C G Smith and M C Payne on one-dimensional ballistic transport experiments and theory. Experimental evidence of the effects described above will be published separately.

Appendix. Details of the calculation

The matching of the wavefunction and its derivative in the linear potential drop model requires the evaluation of the Airy functions of argument $-\xi z_0$ and $\xi(L - z_0)$. If we denote by A_1, B_1, A_1', B_1', the Airy functions of the first and second kind, and their first derivative with respect to the argument $-\xi z_0$, and equivalent terms with subscript 2 for the argument $\xi(L - z_0)$, then

$$t = (2\mathrm{i}k\xi/\pi)\exp(-\mathrm{i}k'L)/[-(C_3 - kk'C_2) + \mathrm{i}(k'C_1 - kC_4)]$$

where $C_1 = \xi(A_2B_1' - A_1'B_2)$, $C_2 = (A_1B_2 - A_2B_1)$, $C_3 = \xi^2(A_2'B_1' - A_1'B_2')$ and $C_4 = \xi(A_1B_2' - A_2'B_1)$. For the case where there is an added potential step, we merely shift the arguments of the Airy functions, as described in the text.

In the case of the smooth potential, the methodology of Landau and Lifshitz (1977) is used, and with a series of definitions and substitutions:

$$\xi = \tanh \alpha z \qquad k^2 = 2m^*E/h^2 \qquad k'^2 = 2m^*(E + V_0)/h^2 \qquad \varepsilon = \mathrm{i}k/\alpha$$

the wavefunction (for $z > 0$) with the correct asymptotic value of $\exp(\mathrm{i}k'z)$ for $z \to \infty$ is

$$\psi(z) = (1 - \tanh^2 \alpha z)^{-\varepsilon/2}\, F[-\varepsilon - s, -\varepsilon + s + 1, -\varepsilon + 1, 0.5(1 - \tanh \alpha z)].$$

This has to be matched at $z = 0$ to the wavefunction for $z < 0$, namely

$$\psi(z) = \exp(\mathrm{i}kz) + r\exp(-\mathrm{i}kz).$$

With

$$\mathcal{F}_1 = F(-\varepsilon - s, -\varepsilon + s + 1, -\varepsilon + 1, 0.5)$$

$$\mathcal{F}_1' = [\alpha(\varepsilon + s)(-\varepsilon + s + 1)/2(-\varepsilon + 1)]F(-\varepsilon - s + 1, -\varepsilon + s + 2, -\varepsilon + 2, 0.5)$$

the transmitted current is given by $(k'/k)\,|2/(\mathcal{F}_1 + \mathcal{F}_1'/ik)|^2$.

Note added in proof. The negative differential resistance has been obtained numerically for the wide–narrow–wide device geometry of Szafer and Stone (1988) and by Shent *et al* (1989, 1990).

References

Brown R J, Kelly M J, Pepper M, Ahmed H, Hasko D G, Peacock D C, Frost J E F, Ritchie D A and Jones G A C 1989 *J. Phys.: Condens. Matter* **1** 6285–90

Kelly M J, Brown R J, Smith C G, Wharam D A, Pepper M, Ahmed H, Hasko D G, Peacock D C, Frost J E F, Newbury R, Ritchie D A and Jones G A C 1989 *Electronics Letters* **25** 992–3

Kirczenow G 1989 *J. Phys.: Condens. Matter* **1** 305–9

Landau L and Lifshitz E M 1977 *Quantum Mechanics, Course on Theoretical Physics* vol. 3, 3rd edn (New York: Wiley) p 80

Landauer R 1981 *Phys. Lett.* **85A** 91–3

—— 1985 *Localisation, Interactions and Transport Phenomena* ed. B Kramer, G Bergmen and Y Bruynserade (Berlin: Springer) p 38–49

Shent C, Sireprakasan S and Kirkner D J 1989 private communication

—— 1990 *Proc. 6th Int. Conf. Hot Carriers in Semiconductors (Phoenix, AZ); Solid-State Electron.* to appear

Szafer A and Stone A D 1988 *Phys. Rev. Lett.* **62** 300–3

Thornton T J, Pepper M, Ahmed H, Andrews D and Davies G J 1986 *Phys. Rev. Lett.* **56** 1198–201

Van Wees B J, Van Houten H, Beenakker C W J, Williamson J G, Kouwenhoven L P, Van der Marel D and Foxon C T 1988 *Phys. Rev. Lett.* **60** 868–70

Wharam D A, Thornton T J, Newbury R, Pepper M, Ahmed H, Frost J E F, Hasko D G, Peacock D C, Ritchie D A and Jones G A C 1988 *J. Phys. C: Solid State Phys.* **21** L209–13